Sol-Gel Method Synthesis and Characterization of Mn doped ZnO Semiconductor Nanostructures for Optoelectronic Devices

By

Assefa Eba Gurara

January 2017

Sol-Gel Method Synthesis and Characterization of Mn doped ZnO Semiconductor Nanostructures for Optoelectronic Devices

By

Assefa Eba Gurara

Submitted in partial fulfillment of the requirements for the degree of Master of Science in physics in School of Applied Natural Science at Adama Science and Technology University

Advisor

Dr. Megersa Wodajo Shura

January 2017
Adama, Ethiopia

ADAMA SCIENCE AND TECHNOLOGY UNIVERSITY POSTGRADUATE PROGRAM

SCHOOL OF APPLIED NATURAL SCIENCEAPPLIED PHYSICS PROGRAM

As thesis research advisor, I hereby certify that I have read and evaluated this thesis entitled: "**Sol-Gel Method Synthesis and Characterization of Mn doped ZnO semiconductor nanostructures for Optoelectronic devices**" Prepared under my guidance by Assefa Eba Gurara. I recommend that it can be submitted as fulfilling the thesis requirement.

Dr. Megersa Wodajo _____ _____

Advisor Signature Date

As the members of the Board of Examiners of the M.SC Thesis Open Defense Examination, we certify that we have read and evaluated the thesis work prepared by Assefa Eba Gurara and examined that the candidate. We recommended that the thesis be accepted as fulfilling the thesis requirement for the degree of Master of Science in Physics.

Name	**signature**	**date**
_____	_____	_____
(Advisor)		
_____	_____	_____
(Program chairman)		
_____	_____	_____
(External Examiner)		
_____	_____	_____
(Internal Examiner)		

DECLARATION AND STATEMENT OF THE CANDIDATE

First, I declare that this thesis is my original work and all sources of materials used for the thesis work have been accordingly acknowledged. This thesis has been submitted in partial fulfillment of the requirements for MSC Degree in Physics at the ASTU and is deposited at the University Library to be made available to borrowers under rules of the Library.

I soberly declare that this thesis work is not submitted to any other institution anywhere for the award of any academic degree, diploma, or certificate.

Brief quotations from this thesis are allowable without special permission provided that accurate acknowledgement of source is made. Requests for permission for extending quotation from or reproduction of this manuscript in whole or in part may be granted by the head of major department or the dean of the school of graduate studies when in his or her judgment the proposed use of the materials is in the interests of scholarship. In all other instances, however, permission must be obtained from the author.

Candidate`s name: Assefa Eba Gurara Signature_____

Place: Adama Science and Technology University, Adama

Date of Submission: January, 2017

ACKNOWLEDGEMENTS

First of all, I would like to be grateful to my advisor Assistance Professor Dr. Megersa Wodajo, for his professional advice, patience and faithful to help me from the beginning to the end of my study in the program of material science by giving me constructive comments and useful suggestions. Once again, I would like to express my sincere gratitude to him for his valuable guidance, inspiration and great material support throughout my entire thesis work. Indeed, without his great dedication, the development and completion of this study would have been impossible.

I would also like to extend my heartfelt gratitude to Alemu Kebede (PhD), Tewodros Yirgashewa (PhD) and Abebe Belay (PhD) for giving me valuable knowledge in their respective courses within the past four summers.

I would like to acknowledge Department of Physics Applied Program and Adama Science and Technology University for extending all their supports to accomplish this study.

Moreover, I wish to express my thanks to all physics teachers in Ambo preparatory school for their cooperation in covering periods given to me and school principal, Mr. Teshome Geleta who cooperates me in giving Laptop and moral in the process of writing this thesis.

I extend my deepest and appreciation to Mr. Assefa Bekele for his unreserved supports and giving moral throughout my study of this thesis.

I would also like to extend my profound gratitude to my beloved wife, Fanose Bekele who shared all life burdens during my stay in the graduate studies.

Finally, I have deepest sense of gratitude and humble thanks to my loving children Nimona Assefa and Haweten Assefa for their giving me moral. Last but not least, my heartfelt gratitude goes to Mr. Demeke Tesfaye for his all technical supports to sample characterization at material engineering laboratory, Adama.

This work has been in its present shape with considerable professional and material inputs from different sources. Therefore, it is amazing excitement to me to come to this

final point and to express my deepest appreciation to all individuals and organizations who/which contributed directly or indirectly to this study and the production of this thesis work.

Contents

List of Figures

List of Tables

List of Acronyms

ZnO	Zinc Oxide
Mn	Manganese
Mn doped ZnO	Manganese doped zinc oxide
XRD	X-Ray Diffraction
UV-Vis	Ultraviolet-Visible
SEM	Scanning Electron Microscopy
CBM	Conduction Band Minimum
VBM	Valence Band Maximum
FWHM	Full Width at Half Maximum
E_g	Band gap Energy
eV	Electron volt
keV	Kilo electron volt
nm	Nanometer
LED	Light Emitting Diode
Å	Angstrom
LUMO	Lowest Unoccupied Molecular Orbital
HOMO	Highest Occupied Molecular Orbital
TM	Transition Metal
T	Temperature
c	Speed of light

Abstract

The purpose of this thesis is to study the growth mechanism and optimize the parameters of this method for Optoelectronic devices and to investigate the structure, optical and electrical properties of Mn doped ZnO semiconductor nanostructures in detail by means of X-ray diffraction (XRD) and Ultra violet-visible absorbance spectrophotometer (UV-Vis). Furthermore, a possible synthesis mechanism for undoped and Mn doped ZnO semiconductor nanostructures in solution was proposed and the effect of Mn doping in different concentrations on the morphology, optical and electrical properties of ZnO nanostructures were systematical studied. The effect of Mn doping on optical quality of ZnO nanostructures was also carefully examined. These nanostructures were successfully synthesized by sol-gel method using the chemicals such as zinc acetate hexa-hydrate, manganese (II) chloride hexa hydrate, ammonia solution, citric acid, poly ethyl glycol and distilled water without further purification. The X-ray powder diffraction (XRD) of the samples was characterized by using SHIMADZU XRD 7000 X-ray diffract meter using the principle of Bragg Brentano Geometry, with Cu-K_{α} radiation. XRD confirmed that all the synthesized undoped ZnO and Mn doped ZnO nanostructures were crystalline in the wurtzite structure; and the average sizes of the samples were investigated, which conform nanostructures' formation. Additional peaks were also observed for Mn doped ZnO nanostructures in this study. UV-Vis absorption spectra were recorded by using a UV-Vis spectrophotometer in the photon wavelength range between 300 and 800 nm. From the optical study, the absorbance in UV regions was increased with the increasing Mn doping concentration. For Mn doped Zn nanostructures, the spectra of U-V show a blue shift in energy band. It was found that the doping of Mn^{2+}ions have a significant influence on the optical properties of ZnO nanostructures.Analyzing the results of various types of characterizations, it has been assessed that Mn doped ZnO nanostructures were successfully synthesized.

Chapter 1

Introduction

The present world is surmounting on the basis of science and technology which include electronics that are mostly dominated by suited electronic equipments. These are creating the need for materials possessing flexible properties. After searching for the history of a material with flexible properties, semiconductor is come out as a common material of this type. Then after the products of semiconductor industry were spreading over the world and deeply penetrating into every activity of human life. As a result, the semiconductor industry has been kept growing tremendously throughout the world. The starting point of semiconductor industry was traced back to the invention of the first semiconductor point contact transistor by Bardeen and Brattain at Bell Lab in 1974 [1] which was further modified by William Shockley [2].

This transistor was manufactured from germanium, which prevents the surface from electrical leakage due to its lower melting point and poor oxides. These properties have imposed major limitations to the application of germanium for device fabrication. As a result, silicon (Si) has been come to use to fabricate discrete devices and integrated circuits for computing, data storage and communication during the development of the information age. It also possesses better fabrication technology and application to integrate circuits for different purposes than germanium. Because of these reasons, it dominates the commercial market at this time [3]. It is a narrow band gap and an indirect band gap semiconductor. Materials with indirect band gaps generate phonons (or heat) during optical emission. Thus, silicon based materials are unsuitable for optoelectronic device, where a direct band gap is needed for efficient optical emission. In addition, its smaller band gap limits its use in applications requiring higher operating temperatures. These limitations have led to the invention of a second generation of semiconductors, namely the III-V compound semiconductors [4].

As time goes on, the rapidly growing world needs speeding up technology. This need is fulfilled by III-V compounds which are more suitable than silicon for high speed-devices

and optoelectronic applications. Among these materials, gallium arsenide (GaAs) is a direct band gap semiconductor possessing higher carrier mobility and higher effective carrier velocity which makes it suite for optoelectronic applications. But this does not complete the requirement of the future world, which needs high temperature electronic devices. Therefore, the world now needs materials that possess unique properties such as larger band gap, higher electronic mobility and higher breakdown field strength. As the development of information technology is going on, the requirement of high power, high temperature electronics and ultraviolet (UV)/ blue light emitter applications became more and more, which is beyond the limitation of silicon or gallium arsenide (GaAs). Because these properties are absent in gallium arsenide. Therefore, wide band gap semiconductors such as SiC, ZnO and GaN that belong to the third-generation semiconductor come forth and turn the researcher focus in the field of semiconductors [5]. Wide band gap semiconductors have gained much attention during the last decade because of their possible uses as optoelectronic devices in the short wavelength and ultraviolet (UV) portion of the electromagnetic spectrum.

Over the last two decades, science and technology have been extremely improved in presenting the true secrets of the nature in molecular or atomic level [6, 7]. In 1959, Richard Feynman gave lecturer titled “There is plenty of room at the bottom”, suggesting the possibility of manipulating things at atomic level which was the basis for the importance and starting of nanomaterials [8]. Systematically, conducting experiments on nanomaterials were seen started from the time of well-known Faraday`s experiments in 1857 [9]. These all together were generally considered as the forecasting of nanotechnology. However, the real burst of nanotechnology did not come until the early 1990s. Device miniaturizations in semiconductor industry as well as the increasing availability of methods of synthesis and tools of characterization and manipulation for nanomaterials were significant factors for the development of nanotechnology [10-12].These characterization tools include sophisticated instruments such as scanning electron microscopy, transmission electron microscopy and electron microscopy, which make researcher approach the nano world [13]. These all together gave birth to a new

branch of science and technology called Nanoscience and Nanotechnology. As a result, nanotechnology was emerging as one of the important disciplines in which physics, biology and chemistry really overlap with one another and has been recognized as a revolutionary of science and technology.

1.1 Background of the study

Nanotechnology is a technology that primarily deals with the synthesis, characterization, exploration and exploitation of nanostructure materials with structural features in between their atoms and their bulk materials [12]. In other words, it is a technology of design and application of nanoscale materials with their fundamentally unique properties and functions. The applications of nanotechnology have got attraction in the areas such as medical, biomedical, healthcare, life sciences, agricultures, safety of food, security, consumer goods, energy production, energy conversion, energy storage, infrastructures, building, construction, aerospace and *etc*. [14-17]. It also provides higher efficiency of devices, new approaches to diagnosis and treatment of diseases; effective environmental monitoring and alternative ways for substantial energy development for a better world [18]. Moreover, its applications also provide very fast response, low-cost, long-life and easy to use by unskilled users. This brings revolution in the life style and safety of human kind. Therefore, it is possible to say that nanotechnology is applied almost in every aspect of our present world.

Nanomaterials are materials that are characterized by at least one dimension in the nanometer (1nm to 100nm) scale. These materials possess the structures known as nanostructures which constitute a bridge between molecules and infinite bulk systems. Structures and sizes have definite effects on the properties of nanoparticles [19]. As a result, the properties of nanomaterials are significantly different from those of a single atom (molecule) and those of bulk matter with the same composition. In line with this, they have also more mechanical strength, thermal stability, catalytic activities, magnetic properties, optical properties, *etc*. than that of the bulk one [20]. The uniqueness of the structural characteristics, energetic, response, dynamics and chemistry of nanostructures constitutes the basis of nanotechnology. A suitable control of the properties and response

of nanostructures can lead to the development of new devices and technologies [12]. Moreover, when the size of materials is in the nanoscale regime, the large surface area to volume ratio exhibited by them improves their high surface reactivity with the surrounding environment. This property makes nanomaterials suitable candidates for many optoelectronic applications. Therefore, nanomaterials have opened up possibilities for new innovative functional devices and technologies [21, 22].

But there are some challenges that face by any researcher while dealing with nanomaterials. These are means to achieve monodispersity, controlling of size and shape, reproducibility, scale up and building complex nanostructures. These challenges can be solved by controlling the variation of PH value, temperature, concentration of reagents, concentration of catalyzer and phase transition (sol-gel method). These are the prime requisites for obtaining quality nanomaterials if they are properly controlled.

In recent years, nanomaterials-based optoelectronics have attracted much attention from both scientific research communities and industrial applications points-of-view. The most important factors for the development of optoelectronic based devices are the fabrication processes which are on economic oriented approach, use of inexpensive materials by economical synthesis methods and require low power consumption, ease of fabrication, high accuracy, fast response time, high compatibility, portable and easy to use by unskilled users.

In the response to above requirements, metal oxide semiconductor nanomaterials have attracted high interest due to their promising applications in diversity of technological areas such as optoelectronic industries, sensing areas, etc. In the fields of nanotechnology based optoelectronics, sensing etc., metal oxides nanostructures stand out as being among the most versatile nanomaterials because of their excellent physical and chemical properties [23, 24]. Among metal oxide nanomaterials, ZnO nanostructures are the most promising metal oxides due to their attractive physical and chemical properties as well as their low-cost, simplicity, environmental friendliness and easy to grow. ZnO nanostructure is highly attractive from research communities in the applications of modern optoelectronic technologies due to its relatively large surface area to volume ratio, thermal

stability, larger band gap of 3.37 eV at room temperature, high exciton binding energy of 60 meV as compared to 28 meV for GaN, which makes exciton in ZnO stable up to 350 K, high transparency, its high ionicity and biocompatibility [23-31]. Its higher band gap ensures a higher breakdown voltage, ability to sustain large electric field, lower electric noise and higher temperature and higher power operation and because of its high exciton binding energy, optically pumped lasing at and above room temperature has been confirmed. It is also an important multifunctional material that appropriates for many different applications in transparent electronics, solar cell, smart windows, bio-detection, piezoelectric devices [32-35].

The properties of ZnO nanostructure can further be tuned by using different ways for improving their applications in optoelectronic and electronic devices. One way is doping method, which intentionally introduces impurities into an extremely pure intrinsic semiconductor for the purpose of modulating its electrical properties. It is a widely-used method to improve the electrical and optical properties of this material. Doping of Mn into ZnO offers an interesting way to alter various properties, for example, the band gap of the host material can be tuned from 3.37 eV to 3.70 eV [36]. The doping of manganese was chosen due to its ionic radius (0.66Å) comparable with ionic radius (0.6Å) of Zn^{2+} and ease to synthesis without changing the ZnO crystalline structure over a wide range of dopant concentration. Moreover, it is known that manganese incorporated into ZnO lattice to form an impurity energy level and facilitate mobility of charge carriers [37]. Additionally, it also alters the emission properties by providing an efficient channel for the recombination of electron and hole via the dopant Mn d levels. Thus, dopant influences the properties of ZnO nanostructures such as the band gap, optical property and electrical conductivity [38]. Therefore, it is clear that ZnO and its ternary alloys have potential to compete with III-V Nitrides for optoelectronic applications. Besides, the possibilities of band gap tuning by forming $Zn_{x-1}Mn_xO$ alloys from zinc oxide nanostructures have also attracted some attention. A systematic study on the influence of manganese ion doping degree on the structure, electrical and optical properties of ZnO nanostructures has been reported in this work.

However, synthesis route is also very important to get different types of nanostructures with different properties. Moreover, the effect of Mn ions on the size and the properties of ZnO can also be analyzed by changing the concentration of Mn ions in these nano structures. Growth conditions and synthesis method for undoped ZnO and Mn doped ZnO nanostructures have already been reported by other researchers [39] were further optimized and studied in detail.

Undoped ZnO nanostructures can be prepared on large scale by low cost, simple solution-based methods such as chemical precipitate [18], sol-gel synthesis [4, 40]and hydrothermal reaction [41]. The sol gel method has several advantages over other growth processes such as use of simple equipment, low cost, catalyst-free growth, large area uniform production, environmental friendliness and less hazardous. This method has also been successfully employed to synthesize Mn doped ZnO nanostructures. The properties of these materials such as structural, optical, electrical, shape and size can be controlled via the sol-gel method by adjusting the reaction temperature, time and concentration of precursors [31]. The present study is focused on the sol-gel synthesis of $Zn_{1-x}Mn_xO$ (x=0.00, 0.02, 0.04 and 0.06) nanostructures. $Zn_{1-x}Mn_xO$ nanostructures synthesized through sol-gel method were characterized using X-ray diffraction (XRD) and UV-visible spectrophotometer. Therefore, the properties of Mn doped ZnO nanostructures depend on their synthesis route, size, shape, electrical and optical properties along with their corresponding electrical and optical applications in optoelectronics were studied in this work.

In this regard, the optimization methods for Mn doped ZnO nanostructures has paved the way in creating new opportunities for the development of nanostructures based devices like optoelectronic devices. Thus, tailoring the synthesis and characterization of Mn doped ZnO semiconductor nanostructures for optoelectronic devices is the high interest of this study. The synthesized Mn doped ZnO nanostructures with controllable shape, size and structure provides excellent prospects for designing nanotechnology based devices. Thus, the study of synthesis and characterization of Mn doped ZnO nanostructures is also another important work of this study.

Great progress has been made in synthesis methods and device applications of ZnO nanostructures [1, 42-44], however, there are still significant challenges that have to overcome so as to produce efficient ZnO optoelectronic devices. These include understanding the residual n-type conductivity in unintentionally doped ZnO and controlling native defects, visible emissions and possible compensation processes. Apart from the difficulty in achieving n-type conductivity from all types of undoped ZnO and Mn doped ZnO materials (bulk and nanostructures); the reproducible growth of nanostructures is another issue which has attracted considerable attention. It is widely recognized that the structure of undoped ZnO and Mn doped ZnO nanostructures is highly sensitive to the growth of environment such as temperature, precursors and their concentrations, the II/VI ratio or PH value, etc. This sensitivity makes it very difficult to control the growth process for the reproducible formation of a desired structure over large areas. However, in order to fully realize undoped ZnO and Mn doped ZnO based optoelectronic devices, optimized growth method and materials processing techniques have developed in this study. Therefore, the present work is motivated by the above and aimed at obtaining optimized growth conditions for undoped ZnO and Mn doped ZnO nanostructures synthesis by sol gel method and the investigation of optoelectronic properties for nanostructures.

1.2 The objective of the study

The general objective of this research is to optimize the sol gel synthesis and characterization of undoped ZnO and Mn doped ZnO semiconductor nanostructures as well as their uses in optical electronic devices.

The specific objectives of this study are to:

- Synthesize undoped ZnO and Mn doped ZnO nanostructures by sol-gel method and optimize the parameters of this method.
- Characterize the crystalline structure and particle size of the synthesized undoped ZnO and Mn doped ZnO nanostructures using X- ray diffraction (XRD).

- Characterize the optical properties of the synthesized undoped ZnO and Mn doped ZnO nanostructures using Ultraviolet-visible (UV-Vis) spectrophotometer.
- Identify the use of undoped ZnO and Mn doped ZnO nanostructures in optoelectronic devices.

1.3 The organization of the study

The research consists of five chapters: Chapter 1 deals with Introduction, Background, Objective and Organization of the study. Chapter 2 provides Literature review of the paper, chapter 3 presents the synthesis methods of undoped ZnO and Mn doped ZnO nanostructures along with their characterization techniques, chapter 4 presents the results and discussions and chapter 5 is giving research summary and recommendation.

Chapter 2

Literature Reviews

2.1 Classification and synthesis of nanomaterials

Over decades, the ability to tune the structure of semiconductors with near atomic scale has led to further idealization of semiconductor structures: quantum wells, wires, and dots. According to their basic dimensions (X, Y and Z) in space, nanostructures of nanomaterials can be classified into zero-dimension (0-D), one-dimension (1-D), two-dimension (2-D) and three-dimension (3-D). While 0-D nanostructures refer to quantum dots or nanoparticles, 1-D nanostructures refer to nanowires, nano rods, nanofibers, nano belts, and nanotubes, 2-D nanomaterials represent for nano sheets, nano walls and nano plates and 3-D nanomaterials are nano flowers and other complex structures such as nanotetrapods [45-50]. Since quantum effects dominate the properties of the nanomaterials, the density of states (it describes the relationship between states and energy in the band diagram of the materials) of nanomaterials is quite different from that of the bulk materials. The electronic densities of states versus energy in the band diagram for 0-D, 1-D, 2-D and bulk materials are shown in Figure 2.1.

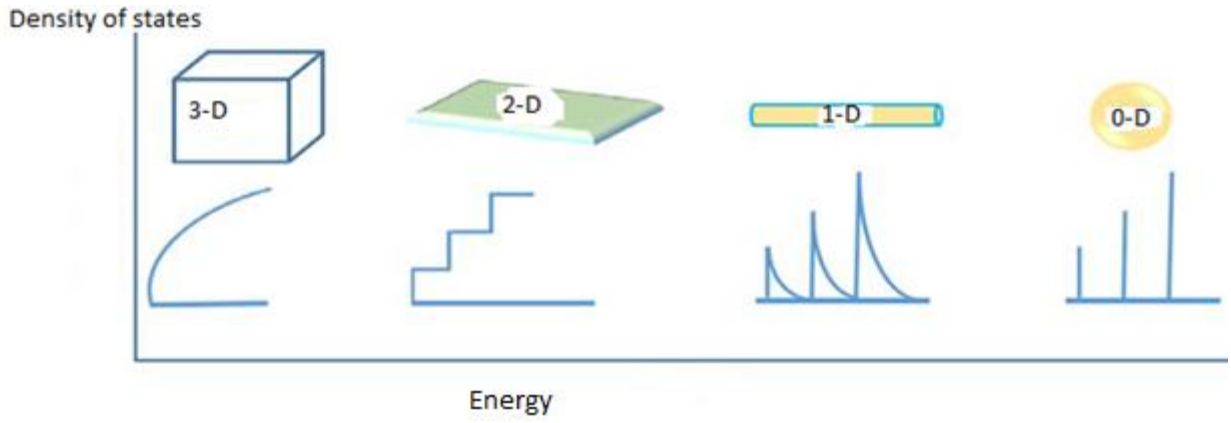

Figure 1: Densities of states in bulk semiconductor and in quantum well (2-D), in quantum wire (1-D), and in quantum dot (0-D) nanomaterials [45, 50].

From the Figure 1 above, one can conclude that the continuous states of bulk materials change to a series of discrete states of nanomaterials.

The syntheses of nanoscale materials are generally grouped into mainly two approaches, namely bottom-up and top-down approaches. The top-down technique is a method that tears down larger building blocks into finer pieces till their constitution up to nanoscale level. In other word; it begins with a pattern generated on a larger scale and then reduces to nanoscale. By nature, it is not cheap and quick to manufacture as well as it is also a slow and not suitable for large scale production. The bottom up method is a method that builds nanomaterials from atomic or molecular precursors. It also starts with atoms or molecules and builds up to nanostructures. It is cheap, fast and suitable to manufacture large scale production. Thus, nanostructures can be synthesized either by bottom-up or top-down approaches. In this research, we have used bottom-up technique to synthesis nanostructures, particularly undoped and Mn doped ZnO nanostructures. This technique is used due to its cheapness, fastness and suitability. The schematic diagram for the two approaches was summarized in Figure 2 below.

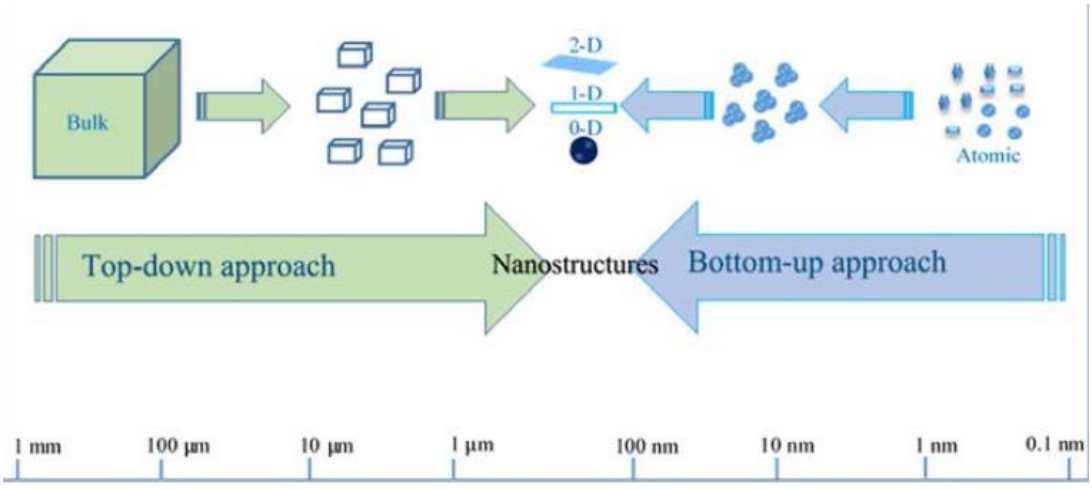

Figure 2: Top-down and bottom-up approaches [50].

2.2 Band structure in nanomaterials

Nanomaterial semiconductors have been widely studied for last several years due to their size dependent physical and chemical properties [51] below critical size characteristics of the materials. Sizes dependent shift in the optical spectrum, luminescence and non-linear optical effects are some attractive properties shown by these nanomaterials. All these variations are seen because of the so called size quantization effects which arise due to the increasing in quantum confinement of the electrons and holes with diminishing size of the crystallites and the subsequent changes in the electronic structures. The structures of these materials give rise to the modifications of their physical properties, particularly to the shift in optical absorption and emission which results in widening in energy gaps as shown in Figure 3 below.

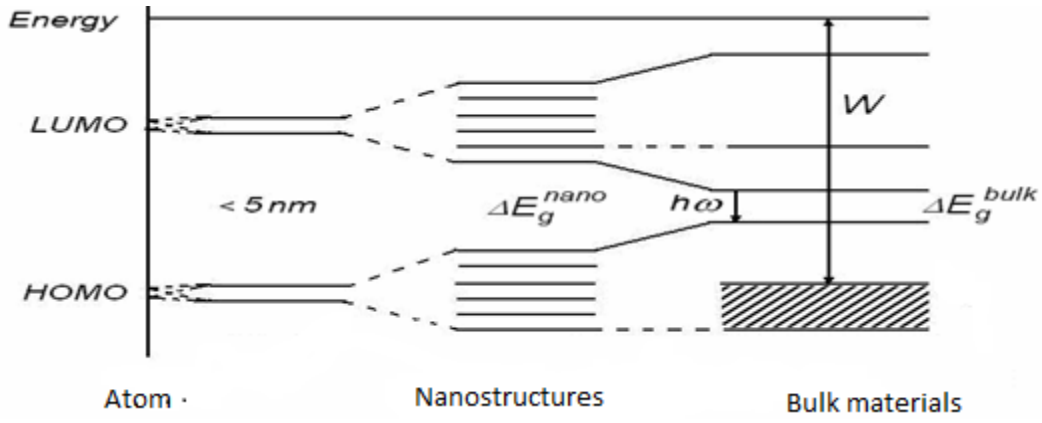

Figure 3: Energy level diagrams comparing of bulk and cluster nanoparticles of semiconductors [51].

Transformation of zone structure of a solid under reduction of its size from macro- to nano-scale down to a single atom shows the increase of the band gap ΔE_g and the blue shift $\hbar\omega = \Delta E_g$ for nanoparticles and nanostructures. Here W is a work function, HOMO is the highest occupied molecular orbital; LUMO is the lowest unoccupied molecular orbital. Due to the finite size of the nanocrystal, the continuous energy bands of the bulk crystal convert into a series of discrete states resulting in widening of the effective band gap. This is normally observed through optical absorption studies in which the lowest allowed absorption shifts to the higher energies as the particle size decreases as in

Figure 3 above. The increase in the energy separation between valence band and conduction band is the consequence of quantum confinement effect. In materials, substantial variations of fundamental, electrical and optical properties are observed when the diameter of the nanostructures is comparable or smaller than the diameter of the bulk exciton such that the energy level spacing exceeds the thermal energy k_BT [52].

For a given temperature this occurs at a very large size in semiconductors as compared to metals or molecular crystal, the nearest neighbor interactions are weak and the bands in solid are very narrow and as a consequence not much size variation in optical and electrical properties are observed in the nanocrystal regime. However, in the case of metals, the edge of the band develops first and the center develops last upon decreasing size. Further, the Fermi level lies in center of the band and the relevant energy gap is still very small and at temperatures above a few Kelvin, the electrical and optical properties more closely resemble those of continuum, even in relatively small sizes. In semiconductors, the Fermi level lies in between the two bands which are covalence band and conduction band, so that the edges of the bands dominate the optical and electrical behavior.

2.3 Background of optoelectronic devices

Optoelectronics is the study and application of electronic devices that interact with light. Over the past decades, substantial improvements in the properties of ZnO have been made. Some improvements include the adjustability of its photoluminescence emission band from blue to yellow [53], the increased quantum yield of up to 85% [54]and the stability of its nanoparticles in aqueous solution for biological labeling [55]. These improvements are coupled with the fact that ZnO offers an affordable non-toxic alternative, other photoluminescence semiconductor, have paved the ways for its applications in optoelectronics. Different ZnO nanostructures have been created from hexagonal patterned nano rods [56] to nano propellers [57]. However, one dimension ZnO nanostructures such as nanowires, nano rods and nano ribbons are the most commonly used when dealing with the optoelectronics [58].

Popular applications in optoelectronics include light emitting diodes (LEDs), laser diodes, photo detectors and photo voltaic cells. Optoelectronic devices are electrical-to-optical or optical-to- electrical transducers, or instruments that use such devices in their operation. In other words, optoelectronic devices are devices that convert electrical energy into optical radiation, or vice versa, and those which detect optical signals through electronic processes. They are also essentially electronic in nature and involve light. These devices provide the optical sources and detectors that allow broad band telecommunications and data transmission over optical ranges. In recent years, considerable progress has been made in the fabrication of optoelectronic devices working at different frequency ranges in the visible spectrum from green/blue to the UV regions/spectra using direct wide band gap semiconductors. Direct band gap semiconductors are used in various domains such as plastics, ceramics, glass, cement, rubber, lubricants, paints, ointments, adhesive, sealant, concrete manufacturing, pigments, foods, batteries, ferrites and fire retardants [59].

2.4 Fundamental properties of ZnO

Among inorganic materials, metal oxides such as ZnO play a fundamental role in developing new devices as they present a considerable variety of structures, stoichiometeries, chemical and physical properties that can be tailored to make use of a variety of suitable synthesis techniques. Zinc oxide has become one of the most attractive materials in research due to its wide application in fields ranging from optoelectronics [60], photo-catalysis [61-64] and optics [65, 66] to biology [67] together with its exceptional properties of good stability, biocompatibility and non-toxicity. It is also one of the most important and versatile functional properties due to its wide spectrum of outstanding properties; moreover, its properties can easily be tailored by adding appropriate dopant [1]. ZnO has a direct wide band gap of 3.44 eV at low temperatures and 3.37 eV at room temperature, which enables it to have some applications in optoelectronics like light-emitting diodes, laser diodes and photo detectors. ZnO has relatively large exciton binding energy of 60 meV, which makes it again promising material for exciton effects based optical devices and due to the lack of a center of symmetry in wurtzite structure combined with a large electromechanical coupling, ZnO possesses large piezoelectric and pyroelectric

properties also make ZnO generally use for sensors, transducers and actuators. In addition, ZnO is a biocompatible and bio safe which attracts it for chemical sensor and biosensors applications [26, 68-71]. Moreover, transition metals (TM) doped with ZnO can change its properties. This is due to the fact that TM-doped ZnO have intrinsic donor defects which contributes to carrier and optical property, which makes TM-doped ZnO useful for optoelectronic applications [68, 70-77]. Furthermore, ZnO possesses different nanostructures such as nano tubes, nanowires, nano rods, nano belts, nanotetrapods, nanoribbons, nano rings, nanocombs which made ZnO nanostructures to possibly be grown on cheap and flexible substrates as well as without substrates. Hence, ZnO nanostructures are attractive and promising material for some future nanotechnology applications [78-80]. However, most of these advantages are definitely utilized due to the fundamental properties of ZnO nanomaterials. Therefore, the basic properties of ZnO and TM-doped ZnO nanostructures, particularly Mn doped ZnO nanostructures were introduced in this study.

2.4.1 Crystal structure and chemical binding

ZnO is an n type semiconductor whose ionicity resides in between being covalent and ionic semiconductor. The crystal structures of ZnO are wurtzite (*B4*), zinc blended (*B*3), and rock salt (*B1*). However, under ambient conditions, the thermodynamically stable phase is the wurtzite [42, 70]. ZnO crystallizes usually in the hexagonal wurtzite type structure shown in Figure 4. In this phase, the ZnO has a polar hexagonal axis called the c-axis that is parallel to the z-axis. The primitive translation vectors $\boldsymbol{a}$ and $\boldsymbol{b}$ with equal length lay in the x-y plane which makes an angle of 120° and the primitive translation vector $\boldsymbol{c}$ is parallel to the *z-axis* [81]. At room temperature, the wurtzite structure has a hexagonal unit cell with lattice parameters $a = b \approx 0.3249$ nm and $c \approx 0.5206$ nm and the ratio c/a value is around 1.603, which is slightly different from the ideal value $c/a = 1.633$ for hexagonal structure. The point group is 6 mm or C6v and the space group is P63mc in Hermann–Mauguin notation and in Schoen flies' notation [42, 81, 82]. Every atom of one kind (group II atom) is surrounded by four atoms of the other kind (group VI), or vice versa, which means that one zinc ion (cation) is surrounded tetrahedrally by four oxygen ions (anions) and vice versa. Its structure is arranged by alternating planes of tetrahedrally coordinated O^{2-} and Zn^{2+}

ions stacking along the c-axis, which makes the entire structure to lack central symmetry. The surfaces can be terminated either with cations or anions, which leads ZnO possesses positively or negatively charged on the surfaces [83].

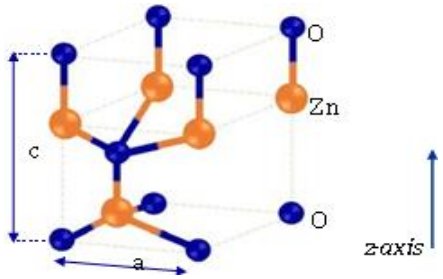

Figure 4: The hexagonal wurtzite of ZnO crystal structure [70, 42, 81, 82]

2.4.2 Basic physical parameter for Wurtzite ZnO

As mention earlier, nanotechnology applications are partly relying on the fundamental properties of the nanomaterials. Therefore, understanding the fundamental physical properties of ZnO is important to the rational design of functional devices. It should be noted that as the dimension of the semiconductor materials shrink down to nanometer scale, some of their physical properties undergo changes due to quantum size effects. However, some of these parameters of ZnO are not well demonstrated, for example, hole's mobility and effective mass are still under debate. Table 1 shows some of the basic physical parameters for wurtzite ZnO [84-87].However, investigation of the properties of individual ZnO nanostructures is essential for developing their nanoscale devices.

Table 1*:* Some basic physical parameters for wurtzite ZnO [18]

Physical parameters			
Lattice parameters at 300 K	a_0	0.32495m	
	c_0	0.52069m	
	c_0/a_0	1.603	1.603 (ideal hexagonal structure 1.633)
Density			5.606 g/cm^3
Stable phase at 300 K			Wurtzite
Melting point			2248 K
Linear expansion coefficient (/^{o}C)			a_0:6.5×10^{-6}
			c_0:3.9 x 10^{-6}
Static dielectric constant			8.656
Refractive index			2.008, 2.029
Energy gap (T=300 K)			3.37 eV (direct band gap)

Intrinsic carrier concentration	$<10^6$ cm^{-3} (max n-type doping$>10^{20}$ cm^{-3} electrons; max p-type doping$<10^{17}$ cm^{-3} holes)
Exciton binding energy	60 meV
Ionicity	62%
Electron effective mass	$0.24m_0$
Electron mobility (T = 300 K)	200 $cm^2/V.s$
Hole effective mass	$0.59m_0$
Hole mobility (T = 300 K)	5-50 $cm^2/V.s$

(m_o is the mass of free electron)

2.4.3 Band structure of Wurtzite ZnO

The band structure is a very important property of a semiconductor, because many important properties and parameters are derived from it, e.g. band gap and effective masses of electrons and holes. For this reason, understanding of the band structure of ZnO is crucial to explain the electrical properties, optical properties and many other phenomena. The band structure provides the electronic one-particle (i.e. electron or hole) states. ZnO is a direct band gap semiconductor which crystallizes in the wurtzite symmetry because the uppermost valence band (VB) and the lowest conduction band (CB) are at the same position in the Brillion zone, namely at k=0 which means the change in momentum is zero, i.e. at the Γ-point [82, 88]. The lowest CB is formed from the empty 4s states of Zn^{2+} or the anti-binding sp^3 hybrid states and the VB originates from the occupied 2p orbital of O^{2-} or the binding sp3 orbital. Under the crystal field and spin orbit interaction, the valence band is split into three sub VB of symmetries, which are labeled in all wurtzite type semiconductors from high to low energies as A, B, and C bands. In most cases, the ordering of the bands is $A\Gamma_9$, B Γ_7, C Γ_7. However, for ZnO there is a long debate whether the ordering as usual or A Γ_7, B Γ_9, C Γ_7. Therefore, the ordering A Γ_7, B Γ_9, C Γ_7 have been selected [82, 88, 89] as shown Figure 5 below and A Γ_7, B Γ_9 and C $\Gamma_7$correspond to heavy holes, light holes and split-off holes respectively. This implies that A and C possess Γ_7 symmetry and B has Γ_9 symmetry. The relation between the energy band gap (E_g) and temperature (T) dependence up to 300 K is given by:

$$E_g(T) = E_g(0) - \frac{(5.05 \times 10^{-4})T^2}{T + 900}. \quad (1)$$

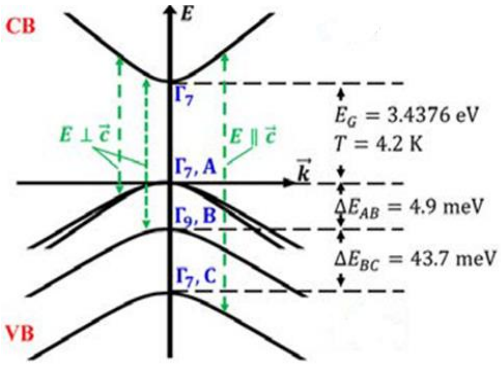

Figure5: The valence band (VB) and conduction band (CB) of ZnO nanostructures [82, 88, 89].

2.4.4 Electrical properties of ZnO

Undoped ZnO semiconductor often shows n-type conductivity due to its native defects such as oxygen vacancies and zinc interstitials [87]. As mention earlier, ZnO semiconductor material is a direct wide band gap material with a relatively large exciton binding energy, which is attractive for many electronic and optoelectronic applications. Because of wide band gap, materials may have high breakdown voltages, lower noise generation, ability to sustain large electric fields, and they can operate at high temperature with high power. The electron transport in ZnO is different at sufficiently low and high electric fields [42, 70]. When low electric field is applied, the energy gained by the electrons from the field is small as compared to the thermal energy of electrons. Hence, the energy distribution of electrons in the ZnO is unaffected by applying low electric field. Therefore, the electron mobility remains constant because the scattering rate indicates that the electron mobility remains independent of applied low electric fields, and Ohm's law is obeyed [42, 70]. When the electrical field is increased to a point that the energy of electrons from the applied electrical field is no longer negligible compared to the thermal energy of the electron, then the electron distribution function changes significantly from its equilibrium value and these electrons become hot electrons with higher temperature than the lattice temperature. Therefore, there is no energy dissipated to the lattice during a short and critical time and when the drift velocity of an electron is higher than its steady-state value, a higher frequency device is possible to fabricate [42, 70].

2.4.5 Piezoelectric properties of ZnO

The mechanical properties of materials involve various concepts, including piezoelectric constants. The physical quantity called strain is described as the deformation of solids under the effect of external forces and the physical quantity called stress is described as the internal mechanical force that resists deformation and tends to return the solid to its initial state [42]. Piezoelectric properties are due to the polarization at atomic level. The mechanical strain can affect the charge carrier transport in materials. For a homogeneous material, three mechanisms may alter its transport characteristics, including the geometric change, the piezoresistive effect (changes the material resistivity), and the piezotronics effect [90]. In case of wurtzite ZnO nanostructures, the origin of the piezoelectricity is described as follows: consider an atom with a negative charge that is surrounded tetrahedrally by positive charges, in which the oxygen atoms and zinc atoms are tetrahedrally bonded. When an external force is exerted on the crystal along the direction of the tetrahedron, the center of the positive charge and the negative charge can be displaced due to lattice distortion. This distortion can cause the center of positive charge and negative charge to displace from each other, which induces local dipole moments. If the whole crystals have the same orientation, the crystals will possess macroscopic dipole moments, while it is experiencing the external force or external pressure [79, 86, 87]. The ZnO nanostructure comprises alternating layers of Zn^{+2} and O^{-2} atoms stacking along the c-axis with a lack of center of symmetry in ZnO, leading ZnO to possess a strong piezoelectricity property providing a relatively large electromechanical coupling. This offers significant potential for applications in nano-electromechanical systems, sensor development and electromechanically coupled sensors and transducers [85, 86, 88].

2.4.6 Optical properties of ZnO

The simplest experiment for determining the size dependence of semiconductor nanoparticles is to understand the absorption spectrum of a material as a function of incident photons' wavelength. These photons are absorbed when their energy is equal to or greater than the energy gap of the semiconductor under consideration. Since the optical properties of a semiconductor are related to its intrinsic and extrinsic factors, their

intrinsic optical properties are also related to the relation between electrons in the conduction band (CB) and holes in the valence band (VB), including exciton effects due to the Coulomb interaction. Extrinsic properties are related to dopants or defects introduced in the semiconductor, which generate discrete electronic states between CB and VB [70]. This implies that the optical properties of semiconductor related dopants or defects introduced to them. From this point of view, we conclude that the optical absorption spectra show the size quantization effect and the estimation of the band gap. Optical transitions in ZnO have been investigated by various experimental techniques such as optical absorption, transmission, reflection, photoluminescence, cathodoluminescence, etc.

2.5 Characterization methods

Different characterization techniques were used to gain deep understanding of the morphological characteristics, crystalline, optical property and particle size of the synthesized ZnO and Mn doped ZnO nanoparticles. The most common techniques used in this study were X-ray diffraction (XRD), Scanning and Ultraviolet visible absorbance spectroscopy (UV-Vis). These techniques can be categorized as structural and optical characterizations where structural characterization includes X-ray diffraction (XRD), Scanning electron microscopy (SEM) and Transmission microscopy (TEM) as well as optical characterization includes ultraviolet visible absorbance spectroscopy (UV-Vis) and Photoluminescence (PL) spectroscopy. In line with this, the crystal structure and particle size were determined using XRD and the optical effect was analyzed from the spectra data using UV-Vis spectroscopy. The characterizations of Undoped and Mn doped ZnO nanostructures using these instruments are presented as follows.

2.5.1 X-ray diffraction (XRD)

X-rays are electromagnetic radiations of wavelength 1Å (10^{-10}m) which occur between ultraviolet and gamma rays in the portion of the electromagnetic spectrum. The discovery of X-rays in 1895 enabled scientists to probe crystalline structure at atomic level [5]. X-ray diffraction (XRD) is a rapid, a non-destructive and a powerful technique used to study the phase of a crystalline material, information on unit cell lattice parameters, crystal structure,

crystal orientation and crystallite size [91]. XRD is widely used to characterize unknown crystalline materials. The working principle of the XRD technique is relied on constructive interference of X-rays and a crystalline sample [91]. In a crystal, the atoms distribute regularly in space, which comes into being crystal lattices. These lattices form a series of parallel planes with spacing distance *d*. The x-rays are generated by a cathode ray tube (X-ray produced by the impact of accelerated electrons with heavy metal such as Cu), filtered (filtered and collimated by nickel filters) to produce monochromatic X-ray radiation which is directed toward the sample. When X-ray light with wavelength λ is projected onto a crystal lattice at an angle θ, the interaction of the incident X-rays with the sample provides constructive interference if the conditions satisfy Bragg's law [92]:

$$n\lambda = 2d_{hkl} \sin\theta, \tag{2}$$

where n is an integer 1, 2, 3, … (usually n =1 for consideration of first order), λ is wavelength in angstroms (1.5418 Å for Cu-K_α), d_{hkl} is spacing between the planes called inter planar lattice constant, θ is the angle between the incident light and the lattice planes, the 2θ is angle between the incident and scattered beams, the angle 2θ of maximum intensity is called the Bragg angle. All diffraction directions of the lattice will be generated by scanning through a range of 2θ angles on the sample. Figure 6 illustrates the reflection of X-rays from two planes of atoms in a crystal solid. From these XRD patterns, the lattice parameter of the samples can be estimated by equations 3-4. The direction of plane normal [*hkl*] is perpendicular to a plane of atoms and the diffraction vector **S** is the vector bisects the angle between the incident and diffracted beam [93]. The lattice constants '*a*' and '*c*' and the spacing d_{hkl} for the wurtzite structure of ZnO can be calculated using the relations written below [92-95]:

$$a = \sqrt{\frac{1}{3}}\frac{\lambda}{\sin\theta} \quad \text{and} \quad c = \frac{\lambda}{\sin\theta} \tag{3}$$

The lattice parameter$d_{hkl}$is then given by:

$$d_{hkl} = \frac{ac}{2}\sqrt{\frac{3}{c^2(h^2+hk+k^2)+\frac{3(al)^2}{4}}}. \tag{4}$$

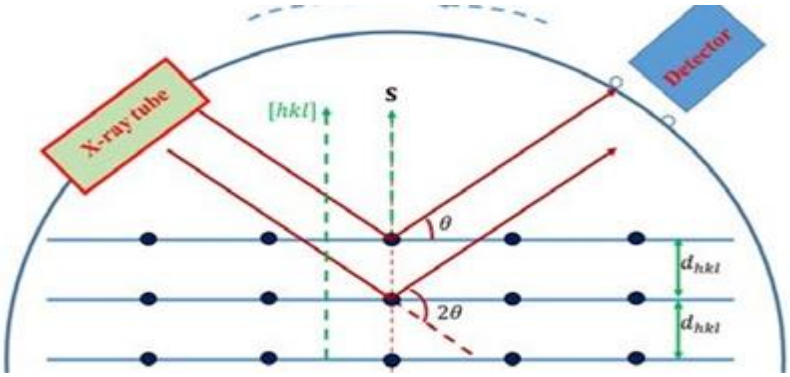

Figure 6: Typically, Bragg Brentano geometry [92-95]

When the size of individual crystals is less than 0.1μm, the term particle size is used. The average crystalline (grain) size of a given sample was calculated using Sherrer formula [96]. The average grain size of a crystalline is calculated from the Sherrer formula as:

$$D = \frac{0.9\lambda}{\beta \cos\theta}, \tag{5}$$

where β is the full width at half maximum of the peak and D is the average grain size of the crystalline. The full width β is usually measured in radians at half of the maximum intensity. It can also be taken as half of the difference between the extreme angle at which the intensity is zero [97, 98].

2.5.2 Ultraviolet Visible Absorption Spectroscopy (UV-Vis)

The electronic band structure of semiconductors and metals is determined by their optical properties. The optical absorption is resulted from the interaction of the material and light. When the frequency of light is in resonance with energy difference between states where the transition allowed or partly allowed by selection rules a photon is absorbed by the material. This results in a decrease of transmission or an increase in absorbance of light passing through the sample. By measuring the transmission or absorbance of sample as a function of the frequency of light, one can obtain a spectrum characteristic of the material [99]. UV-Vis absorption spectroscopy is the measurement of the attenuation of a beam of light after it passes through a sample or after reflection from a sample surface. Absorption measurement can be done at a single wavelength or over an extended spectra range.

Visible and ultraviolet lights are energetic enough to promote outer electrons to higher energy levels and UV-Vis spectroscopy is used to find the absorbance, energy band gaps and intensity over wave length of molecules or inorganic complexes in solution. The UV-Vis spectra have broad features that are of limited use for sample identification but are very useful for quantitative measurements. The concentration sample solution can be determined by measuring the absorbance at some wavelength. The Beer-Lambert law states that the absorbance of a solution is directly proportional to the concentration of the solution [100]. This relation can be expressed as:

$$I = I_0 e^{-A} \; and \; A = \epsilon c b, \tag{6}$$

where A is the measured absorbance, I_0 is the intensity of incident light at a given wavelength and I is the transmitted intensity. Hence, UV-Vis can also be used to determine the concentration of samples in solution. The optical absorption coefficient is determined based on the band gap energy (E_g). The band gap energy of the sample is obtained by using the absorption edge relation [101]:

$$\mathrm{E}_g(\lambda) = \frac{hc}{\lambda}, \tag{7}$$

where h is planck's constantand c is the speed of light. The fundamental absorption method refers to band to band transition using Mott and Davis relation [102] of the equation below. For photon energies just above fundamental edge, the absorption coefficient follows the standard relation:

$$\alpha h\upsilon = A\left(h\upsilon - E_g\right)^n, \tag{8}$$

where A is a constant related to the extent of the band tailing, α is absorption coefficient, $h\upsilon$ is photon energy, E_g is energy band gap which is the energy gap between the valence band and the conduction band and $n = 1/2$ for allowed direct transition, $n = 2$ for allowed indirect transition.

Chapter 3

Materials and Methodology

3.1 Synthesis of nanostructures

The synthesis method has been employed a modified version used by S. Sambassive for [103]. All chemicals for the synthesis of undoped ZnO and Mn doped nanostructures were used as received without further purification. For the synthesis of $Zn_{1-x}Mn_xO$, sol-gel method was used. The dopant concentration 'x' ranges from 0.00 to 0.06, where x=0.02, 0.04 and 0.06 represents 2%, 4% and 6%atw of Mn doped samples respectively.

3.2 Experimental site

The synthesis of undoped ZnO and Mn doped ZnO nanostructures were conducted at Adama Science and Technology University, ASTU Chemistry Post Graduate Laboratory. The characterizations of the synthesized undoped ZnO and Mn doped ZnO nanostructures were made by using X-ray diffraction (XRD) and Ultraviolet (UV)-Visible absorbance spectrophotometer and also done at Adama Science and Technology University, ASTU Chemistry Post Graduate Laboratory and Material Engineering Laboratory.

3.3 Apparatus used

The apparatus used in the experiment were Glass beakers, Volumetric flasks, Magnetic stirrer with hot plate, Magnetic pellets, Thermometer, Electronic balance, Universal Drying Oven, Spatula, Tong, Sample holder, Marker point, Clean and white paper, Muffle furnace and small mortar pestle.

3.4 Chemical used

The chemicals used in this work were purchased from Avi-Chem Industries and used without further purification. While distilled water was used as solvent, zinc acetate hydrate ($Zn(CH_3COO)_2.2H_2O$, 99%), and manganese (II) chloride hydrate ($MnCl_2.4H_2O$, 99%) were used as zinc and manganese precursor sources respectively. Citric acid ($C_6H_8O_7.H_2O$) was

used as passivating agents to attain PH value about 1.5; poly ethylene glycol was used capping agents to stop particles agglomeration; and ammonia solution was put in the result drop by drop until PH value is about 8.

3.5 Methods of sample preparation

The glass beakers were first cleaned and rinsed with distilled water and dried in dry oven. All the chemicals, passivating agent, capping agent and solvent were weighted with the help of electronic balance and mixed them accordingly to the concentrations of manganese. To achieve the required compositions of $Zn_{1-x}Mn_xO$ (x= 0.02, 0.04 and 0.06), appropriate amount (8g) of zinc acetate ($Zn(CH_3COO)_2.2H_2O$) and manganese (II) chloride ($MnCl_2.4H_2O$) was dissolved in 75 ml of distilled water at 70^0c along with 6 ml of poly ethylene glycol and keeping the zinc acetate constant in all reactions. A citric acid was added to this solution drop by drop to attain PH value about 1.5. The resulted solution was continually stirred for 10 minutes until a sol is formed. Then ammonia solution (28%) was added to the above result drop by drop until PH value is about 8. The formed hydrolysis product was continuously stirred for 3 h and then kept at room temperature to form a gel. Finally, the resulted gel was dried in the dry oven for 12 -18 h and then calcined at 400^0C for 2 h in air in muffle furnace to attain nice morphological distribution of the active bend and the calcined samples were then grinded to prepare for characterizations.

Citric acid was used to study the effects of surface passivation on the morphological, crystalline and optical properties. In the case where citric acid was used more fine powders were resulted. It also enhances the crystallization processes at lower temperatures but does not influence the particle size. It also acts as chelating and structural directing agents [102, 104].

3.6 Characterization method for nanostructures

Various techniques can be used for undoped and doped ZnO nanostructures characterization. The most common techniques used in this work were X-Ray Diffraction

(XRD) and Ultraviolet visible spectrophotometer (UV-Vis).Experimental procedures in Sol Gel Method are summarized as follows:

$Zn(CH_3COO)_2.2H_2O$ (8 g) and $MnCl_2.4H_2O$ (The Mn content in the samples is 0.02, 0.04 and 0.06) were dissolved together in 75 ml of distilled water at 70^0C

⇩

Citric acid was added drop by drop to the above solution until PH= 1.5 along with 6 ml of poly ethylene glycol at this temperature.

⇩

Stirred for 10 minutes and then a sol is formed

⇩

$NH_3.H_20$ (28%) is added drop wise to the above sol under magnetic stirring until pH = 8

⇩

The hydrolysis product is stirred for 3 h and then kept at room temperature to form a gel

⇩

This gel was dried at 120^oC for 12-18 h in dry oven

⇩

The dried samples were Calcined at 400^oC for 2 h in air

⇩

Mn doped ZnO nanostructures were synthesized

Figure 7: Steps involved in Sol Gel method to synthesize Mn doped ZnO nanostructures.

The uses and work principles of these techniques are stated as follows.

3.6.1 X-ray diffraction (XRD)

The X-ray diffraction (XRD) pattern for undoped and Mn doped ZnO nanoparticles was obtained using SHIMADZU XRD-7000 system with X-ray diffract meter by generating Cu-K_α radiation (λ=1.5418Å) at Adama Science and Technology University, Material Engineering Laboratory. It is used to determine the crystalline phase of the synthesized nanostructures.

We have used small amount of sample in powder form for characterization under this technique. An X-ray generator was operating at a voltage of 40kV and applied a current of 30mA at room temperature. Intensities were measured at room temperature in steps of 0.02, over the range of $10^0 \leq 2\theta \leq 80^0$, the diffractometer is connected to a computer for data collection and characterization displays. The peaks of the X- ray diffraction pattern can be compared with the standard available data for the confirmation of the structure.

3.6.2 Ultraviolet-Visible spectrophotometer (UV-Vis)

Absorbance spectra were recorded with UV-Vis (T80 +UV/Vis spectrometer PG instruments Ltd) spectrophotometer, using a quartz cuvette of 1 cm path length. Two samples, with one sample contains small amount of undoped ZnO and Mn doped ZnO nano powders each were mixed with methanol and the other contains only methanol, were prepared by keeping their proportional in volumetric flask and was shaking well using mixer for this purpose. The solution in a volumetric flask contained only methanol was poured into quartz cuvette of width 1 cm. It was then put in Ultraviolet visible spectrophotometer to block the effect of this solution on the synthesized undoped ZnO and Mn doped zinc oxide powder soluble in the former sample. Then after the former sample solution was poured into quartz cuvette of 1 cm width and put this cuvette in Ultraviolet visible spectrophotometer to measure the absorbance over the wavelength range of 300-800nm. All spectra were recorded after proper diluting the solution.

Chapter 4

Results and Discussion

Undoped ZnO and Mn doped ZnO nanostructures were synthesized by sol gel method at 120^0c for 12-18 h and calcined at 400^0C for 2hours in air in furnace by keeping the concentration of $Zn(CH_3COO)_2.2H_2O$ as constant in all reactions while the concentration of Mn was varied from 0.02 to 0.06. Reaction mixture attained different colors with different dopant at different stages. In the case where ammonia solution was added to the result solution, it was changed to white then went through a brownish transparent phase. The synthesized undoped ZnO and Mn doped ZnO nanostructures were characterized using X-ray diffraction (XRD) and Ultraviolet-visible absorbance spectrophotometer (UV-Vis). The characterizations of the synthesized samples from XRD and U-Vis spectrophotometer are presented as follows.

4.1 Structural study from x-ray diffraction (XRD)

Figure 8 shows, the powder XRD patterns of $Zn_{1-x}Mn_xO$(x =0.00, 0.02, 0.04 and 0.06) nanostructures synthesized by sol gel technique with subsequent calcinations at 400^0C for 2hours. For undoped and Mn doped (x = 0.02, 0.04 and 0.06) ZnO nanostructures, the patterns show nine different diffraction peaks at scattering angles (2θ) of 31.76, 34.39, 36.23, 47.53, 56.59, 62.84, 66.42, 67.97 and 69.02 degrees corresponding to the reflection from (100), (002), (101), (102), (110), (103), (200), (112) and (201) crystal planes, respectively. All these diffraction peaks can be indexed as hexagonal wurtzite structure of ZnO nanostructures [105]. From this, one can see that XRD patterns indicate the formation of hexagonal wurtzite phase of ZnO for the synthesized nanostructures.

In addition to this, we also found that additional diffraction peaks of other impurity phases (compounds) were observed within the limit of the instrumental sensitivity for the doped samples. These additional peaks are appeared probably due to the presence of Mn_2O_3 (JCPDS No 024-1133). This indicates that the synthesized nanostructures are the mixture of ZnO and Mn_2O_3. The number of the additional peaks is decreasing as the concentration

of Mn doping increases (Figure 8). Peak positions also show measurable change while the relative intensity of the peak increases from 41 to 92 with increasing Mn content from 0.02 to 0.06. These all together suggest that the ZnO lattice changes due to the incorporation of Mn ions into it.

The diffraction peaks of Mn doped ZnO nanostructures are narrowed and shortened as compared to undoped ZnO nanostructure. The average crystallite size of undoped ZnO was calculated to be 18 nm (Table 2). As Mn content increases, the XRD peaks appear to be sharper with decreasing full width at half the maximum (FWHM) intensity. This entire exhibits that the products are well crystallized. The sharp diffraction peaks of Mn doped ZnO nanostructures also suggest that calcinations at 400^0C for 2 h is sufficient to crystallite Mn doped ZnO and show a preferential orientation behavior along (101) lattice plane. The full width at half maximum (FWHM) intensity of the (101) diffraction peak decreases from $0.3367 - 0.2937^0$ with the increasing concentration of Mn^{2+} from 0.02 to 0.06. Therefore, the variation in peaks' width for (101) directions with doping concentration give a clear indication of the change of the average crystallite size of the samples.

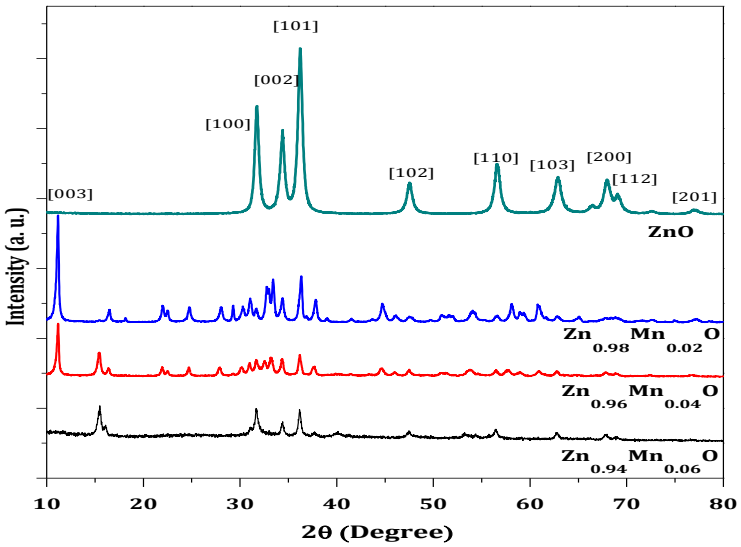

Figure 8: XRD patterns for $Zn_{1-x}Mn_xO$ (x= 0.00, 0.02, 0.04 and 0.06) semiconductor nanostructures.

The average crystallite sizes of the Mn doped ZnO nanostructures were found to be in the range 18-37 nm, which are calculated from equation 5 using the most intense peak (101) plane. The results are summarized in Table 2. With the increasing of Mn

concentration, the average size increases from 32 to 37 nm. This shows, crystallite size increases with increasing concentration of Mn doping, but, with decreasing FWMH intensity. This indicates that, the Mn doped ZnO nanostructures prepared by sol gel method have high crystallite and high purity. The observed inter planer spacing of ZnO can be indexed to hexagonal wurtzite with a value about 0.1149nm (d_{101}). After the addition of doping Mn ions into ZnO lattice, the inter-planar spacing is changed [106].

The inter-planar spacing is 0.1199, 0.1127 and 0.1122nm for the concentration 0.02, 0.04 and 0.06 of Mn doped nanostructures respectively as shown in table 2. These values are calculated using equation 2. It reveals that the Mn ions are successfully incorporated into ZnO lattices side of Zn ions. This substitution is accounted due to the fact that ionic radius of Mn ions (0.66Å) is comparable with or greater than that of Zn ions (0.60Å). The lattice parameter constants 'a' and 'c' are decreasing as Mn concentrations increase (Table 2), which are calculated using equation 3. This decrease is accounted for the fact that ionic radius of Mn ions (0.66Å) is also comparable with or greater than that of Zn ions (0.60Å). Such a change in lattice parameter constants shows the incorporation of Mn into ZnO lattice.

Table 2: Composition, angles of diffraction, FWHM, lattice parameter constants**,** average crystallite size, inter-planar spacing and relative intensity of $Zn_{x-1}Mn_xO$ ($\boldsymbol{x}$=0.00, 0.02, 0.04 and 0.06) nanostructures for (101) peak of diffraction.

Composition (x)	**Diffraction Angle (Degree)**		**FWHM**		**Lattice constants (nm)**		**Grain size (D)**	**Lattice parameter (d)**	**Relative intensity (I/I_0)**
	2θ	θ	Degree	Radian	$a = b$	c	nm	nm	
0.00	36.2293	18.1147	0.5682	0.009912	0.1326	0.2298	18.87	0.1149	100
0.02	36.2032	18.1016	0.3367	0.005874	0.1308	0.2267	32.48	0.1133	41
0.04	36.1946	18.0973	0.3144	0.005485	0.1302	0.2255	33.02	0.1127	47
0.06	36.1862	18.0931	0.2937	0.005123	0.1296	0.2245	37.09	0.1122	92

(FWHM is Full Width at Half Maximum intensity)

The calculated lattice parameter constants were also in agreement with the values reported by G. Murugadoss *et al*. [106]. Therefore, we have analyzed that the Mn doping affects the lattice parameters and average crystallite sizes of the doped ZnO nanostructures. This is due to structural disorders. Some nanoparticles were aggregated

due to the large specific surface area and high surface energy. The aggregation was occurred during the process of drying.

4.2 Optical properties from UV-Vis spectrophotometer.

UV-Vis absorption spectrum of $Zn_{x-1}Mn_xO$ ($x = 0.00, 0.02, 0.04$ and 0.06) nanostructures was recorded using a UV-Vis spectrophotometer in the photon wavelength between 300 and 800 nm. The optical absorption spectra of $Zn_{x-1}Mn_xO$ nanostructures for these samples were shown in figure 9. This figure depicts that; the absorption edge shifts to higher energy/shorter wavelengths with increasing the doping concentration. This indicates a blue shift in band gap with respect to bulk ZnO (3.37 eV at 300K). Similar blue shift in band gap has been reported in the case of undoped ZnO due to the size affect by other writers [106]. This blue shift in band gap is due to the fact that the size of a semiconductor becomes comparable to the Bohr radius of the exciton leading to variations in the properties of the materials quantum confinement [107]. All these spectra show a significant blue shift in the absorption wavelength.

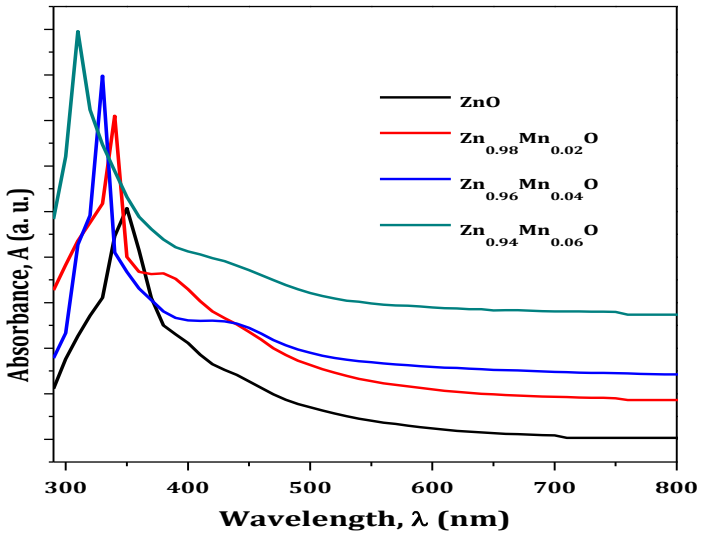

Figure 9: UV-Visible spectra of $Zn_{1-x}Mn_xO$ ($x = 0.00, 0.02, 0.04$ and 0.06) nanostructures.

The change in the band gap has been explained on the basis of a variation of the lattice parameters due to the effect of doping. It has been observed that the energy band gap increases with a decrease in the lattice parameters. This explanation is consistent with our

results that the lattice parameter constants of our nanostructures decrease with increasing Mn doping concentrations.

It can be seen from the above spectra that band gap of material increases appreciably with respect to that of undoped ZnO nanostructures having a band gap of 3.37 eV [108]. The band gap was greatly altered and at different dopant concentrations, x =0.00, 0.02, 0.04 and 0.06. Table 3 below shows the band gap for the un-doped and Mn-doped samples. The values were varied between 3.54 and 3.98 eV as listed in the table. These values were calculated from the UV–Visible spectra using the formula in equation 8. The obtained results were in good agreement with the one that was reported in reference [109] by Shah, S.M *et al*. In addition to the increase in band gap energy, an increase in absorbance was also observed with increasing Mn concentrations (Figure 9).

Table 3: Composition, maximum wavelength and optical band of $Zn_{x-1}Mn_xO$ ($\boldsymbol{x}$=0.00, 0.02, 0.04 and 0.06) nanostructures.

Composition (x)		0.00	0.02	0.04	0.06
Parameters	Maximum wavelength (nm)	351	344	338	312
	Energy band gap (eV)	3.54	3.61	3.68	3.98

Chapter 5

Conclusion and Recommendation

In this work, the synthesis of $Zn_{x-1}Mn_xO$ (x =0.00, 0.02, 0.04 and 0.06) nanostructures using a cost effective, simple and environment friendly method the so called sol-gel method was studied. The obtained results were summarized in this chapter, followed by suggestions for recommendation. Synthesis of $Zn_{x-1}Mn_xO$ nanostructures has been achieved using zinc acetate, manganese (II) chloride, polyethylene glycol and ammonia solution by sol-gel method. In this synthesis route, the chemicals were dissolved by using magnetic stirrer with hot plate and grinding processing has also been mainly carried out as a scalable physical technique to directly break bulk materials to form fine particles. The synthesized undoped ZnO and Mn doped ZnO nanostructures were characterized using XRD and UV-Vis spectrophotometer.

XRD results showed that the obtained undoped ZnO and Mn doped ZnO nanostructures were composed of hexagonal wurtzite phase with very good crystallite and the average crystallite size was found to be 18 nm for undoped ZnO nanostructures. For Mn doped ZnO nanostructures, the average crystallite sizes were found to be varied between 32 and 37nm. This shows that the crystallite size is increasing as Mn doping concentrations increase. Additional peaks were observed for Mn doped ZnO nanostructures. This indicates the presence of Mn_2O_3 and the synthesized nanostructures are the mixture of ZnO and Mn_2O_3.

The lattice parameter constants decrease with increasing the concentration of Mn doping. This indicates Mn ions are incorporated into the ZnO lattice. From this, we concluded that the Mn doping affects the lattice parameter constants and average crystallite sizes of the doped ZnO nanostructures. This is due to structural disorders. From all these points of view, we concluded that undoped and Mn doped ZnO nanostructures prepared by sol-gel method have high crystallite and high purity. Due to the large specific surface area and high surface energy, some nanoparticles were aggregated. The aggregation occurred probably during the process of drying.

Optical absorption investigations were carried out to study the optical quality of $Zn_{1-x}Mn_xO$ nanostructures. The optical absorbance spectra of undoped ZnO and Mn doped ZnO nanostructures were obtained using UV-Vis spectrophotometer. Absorption peak of the spectrophotometer appears at 351 nm for undoped ZnO, which is significantly blue shifted from bulk (370 nm). This is probably due to the size effect. Absorption spectrum peaks for $Zn_{1-x}Mn_xO$ ($x = 0.02$, 0.04 and 0.06) nanostructures are located in the Ultra-violet region at 343, 338 and 312 nm, respectively, which are strongly blue shifted compared to undoped ZnO nanostructures. It may be ascribed to the increase of the particle size by incorporation of Mn^{2+} ions into the Zn matrix. In addition, blue shift absorption of all un-doped and doped samples reveals the increase in the band gap energy. It was found from optical study that the absorbance in UV region was increased with the increase of Mn concentration. For Mn doped ZnO nanostructures, the optical band varies between 3.61 and 3.98 eV. It was also found that the doping of Mn^{2+} ions have a significant influence on the optical properties of Zno nanostructures.

Finally, we summarized that, Mn doping plays a key role in tuning the structural and optical properties of ZnO which in turn improve the applications of ZnO in Optoelectronic devices. This thesis may be used as a base and reference for students who want to study transition metals doped ZnO nanostructures for sensor applications, spintronics and other purposes.

References

[1] C. Jagadish, S.J. Pearton, "Zinc Oxide Bulk, Thin Films And Nanostructures: Processing, Properties And Applications," 2006.

[2] W. Shockley, The Path to the Conception of the Junction Transistor- offprint with inscription and sketch, IEEE Electron Devices Society, 1997, pp. 597-620.

[3] L. Pavesi, "Silicon-Based Light Sources for Silicon Integrated Circuits," *Advances in Optical Technologies,* vol. 2008, pp. 1-12, 2008.

[4] Z.N.Urgessa, "Growth and Characterization of ZnO Nanorods using chemical bath deposition," 2012.

[5] Yang.L, "Synthesis and optical properties of ZnO nanostructures," pp. 1-20, 2008.

[6] J.Fernanddez et al, "CuO, ZrO2 and ZnO nanoparticles as anti-wear additive in oil lubricants.," *Wear,* 2008.

[7] A. H. M. J. A. a. M. Bougrine.A, "Structural, optical and cathodolumuniscence characteristics of undoped and tin doped zinc oxide prepred by spray pyrolysis," *Mater. Chem. Phys,* vol. 80, pp. 438-445, 2003.

[8] I. P. Kaur, V. Kakkar, P. K. Deol, M. Yadav, M. Singh, I. Sharma, "Issues and concerns in nanotech productdevelopment and its commercialization," *Journal of released Release,* 2014.

[9] F. Laeri, F. Schüth, U. Simon, and M. Wark, "Host-Guest-Systems Based on Nanoporous Crystals. Weinheim: Wiley," 2003, p. 435–436.

[10] Gupta.V et al, "Zinc oxide Bulk, Thin Films and Nanostructures," 2006.

[11] Stavola.M, "Identification of defects insemiconductors and semimetals," vol. 51 B, 1999.

[12] Yury Gototsi, "Material science at nano scale," in *Nanomaterial Hand Book*, CRC Press, 2006, pp. 1-21.

[13] He, S.T., J.N., Yao, P.Jiang, D.X.Shi, H.X.Zhang, S.S.Xie, S.J.Pang and H.J.Gao, Lanmuir, 17: 1571-5, 2001.

[14] P. Boisseau, and B. Loubaton, "Nanoscience and nanotechnologies: hopes and concerns nano-medicine, nanotechnology in medicine," *C. R. Physique 12,* pp. 620-636, 2011.

[15] L. A. DeLouise, "Applications of nanotechnology in dermatology," *Journal of Investigative Dermatology 132,* pp. 964-975, 2012.

[16] S. K. Arora, R. W. Foley, J. Youtie, P. Shapira, and A. Wiek, "Drivers of technology adoption- the case of nanomaterials in building construction," *Technological Forecasting & Social Change 87,* pp. 232-244, 2014.

[17] S. Chattopadhyay, L. C. Chen, and K. H. Chen, "Energy production and conversion applications of one-dimensional semiconductor nanostructures," *NPG Asia Mater. 3(6),* Vols. 74-81, 2011.

[18] Chan Oeurn Chey, "Synthesis of ZnO and transition metals doped ZnO nanostructures, their characterization and sensing applications," *Dessertation submitted to Linkoping University, Sweden,* no. 1629, 2015.

[19] Linda Williams Dr. Wade Adams, Nanotechnology Demystified, New york, 2007.

[20] Dr.Ramalingam, "Synthesis of nanomaterials". *power point presentation.*

[21] M. C. Roco, C. A. Mirkin, M. C. Hersam, "Nanotechnology research directions for societal needs in 2020," *summary of international study, J Nanopart Res,* 2011.

[22] C. N. R. Rao, A. Muller, A. K. Cheetham, "The Chemistry of Nanomaterials, WILEY-VCH Verlag GmbH & Co. KGaA, Weinheim," p. 1, 2004.

[23] N. S. Ramgir, Y. Yang, and M. Zacharias, "Nanowire-based sensors, Small," vol. 6, no. 16, pp. 1705-1722, 2010.

[24] L. Vines and A. Kuznetsov, "Bulk Growth and Impurities, Semiconductor and semimetal," *oxide semiconductors,* p. 68, 2013.

[25] P. R. Solanki, A. Kaushik, V. V. Agrawal, and B. D. Malhotra, "nanostructured metal oxide-based biosensors," *NPG Asia Mater,* vol. 3 , no. 1, pp. 17-24, 2011.

[26] Z. L. Wang, and J. Song, "Piezoelectric nanogenerators based on zinc oxide nanowire arrays," *Science,* vol. 312, no. 5771, pp. 242-246, 2006.

[27] B. X. Du, Z. Mei, Z. Liu, Y. Guo, T. Zhang, Y. Hou, Z. Zhang, Q. Xue, and A. Yu.Kuznetsov, "Controlled growth of high-quality ZnO-based films and fabrication of visible-blind and solar-blind ultra-violet detectors," *Adv. Mater,* no. 21, pp. 4625-4630, 2009.

[28] R. Schifano, E. V. Monakhov, U. Grossner, and B. G. Svensson, "Electrical characteristics of palladium Schottky contacts to hydrogen peroxide treated hydrothermally grown ZnO," *Applied Physics Letters,* no. 91, 2007.

[29] V. Venkatachalapathy, A. Galeckas, I. H. Lee, A. Yu. Kuznetsov, "Engineering of nearly strain-free ZnO films on Si (111) by tuning AlN buffer thickness," *Physica B,* no. 407, pp. 1476-1480, 2012.

[30] N.T. Son, I.G. Ivanov, A. Kuznetsov, B.G. Svensson, Q.X. Zhao, M. Willander, M. N.Morishita, T. Ohshima, H. Itoh, J. Isoya, E. Janzen, R. Yakimova, "Common point defects in as-grown ZnO substrates studied by optical detection of magnetic resonance," *Journal of Crystal Growth,* no. 310, pp. 1006-1009 , 2008.

[31] T. Moe Børseth, B. G. Svensson, A. Yu. Kuznetsov, P. Klason, Q. X. Zhao, and M.Willander, "Identification of oxygen and zinc vacancy optical signals in ZnO," *Applied Physics Letters,* no. 89, 2006.

[32] J. E. Stehr, S. L. Chen, S. Filippov, M. Devika, N. K. Reddy, C. W. Tu, W. M. Chen,and I. A. Buyanova, "Defect properties of ZnO nanowires revealed from an optically detected magnetic resonance study,"

Nanotechnology, no. 24, 2013.

[33] S. L. Chen, W. M. Chen, and I. A. Buyanova, "Slowdown of light due to exciton-polariton propagation in ZnO," *Physical Review B,* no. 83, 2011.

[34] W. M. Chen, I. A. Buyanova, A. Murayama, T. Furuta, Y. Oka, D. P. Norton, S. J.Pearton, A. Osinsky, and J. W. Dong, "Dominant factors limiting efficiency of optical spin detection in ZnO-based materials," *Applied Physics Letters,* no. 92, 2008.

[35] M. Willander, L. L. Yang, A. Wadeasa, S. U. Ali, M. H. Asif, Q. X. Zhao and O. Nur, "Zinc oxide nanowires: controlled low temperature growth and some electrochemical and optical nano-devices," *J. Mater. Chem. ,* no. 19, pp. 1006-1018, 2009.

[36] "Synthesis of ZnO : Mn nanoparticles, nano belts and nano rods," *Ovonic Research,* vol. 4, no. 5, pp. 101-105, 2008.

[37] Rosari Saleh , Nadia Febiana Djaja, "Transition-metal-doped ZnO nanoparticles," *Synthesis, characterization and photocatalytic activity under UV light,* pp. 581-590, 24 March 2014.

[38] X. J. Wang, I. A. Buyanova, W. M. Chen, M. Izadifard, S. Rawal, D. P. Norton, S. J.Pearton, A. Osinsky, J. W. Dong, and Amir Dabiran, "Band gap properties of Zn1-x CdxO alloys grown by molecular-beam epitaxy," *Applied Physics Letters,* no. 89, 2006.

[39] A.K.Singh , V.Viswanath,V.C.Janu, "Synthesis, effect of cappingagents,structural,optical and photoluminescence properties of ZnO nanoparticles," *Luminescence,* 2009.

[40] S.Y. Chu, T.M. Yan and S.L. Chen, *J.Mater. Sci. Lett,* vol. 12, no. 349, 2000.

[41] J.H. Kim, W.C. Choi, H.Y. Kim, Y. Kang and Y.K. Park, *Power Technol166,* no. 153, 2005.

[42] H. Morkoc and U. Ozgur, "General properties of ZnO, Zinc Oxide," in *Fundamentals, materials and device technology*, 2009, pp. 1-2.

[43] A.B. Djuris˘ic’ , A.M.C. Ng, X.Y. Chen, "Progress in Quantum Electronics 34," p. 191, 2010.

[44] L. Schmidt-Mende, J.L. MacManus-Driscoll, "Materials Today 10," vol. 5, 2007.

[45] A. P. Alivisatos, "Perspectives on the physical chemistry of semiconductor nanocrystals," *J. Phys. Chem,* no. 100, pp. 13226-13239, 1996.

[46] Y. Zhang, M. K. Ram, E. K. Stefanakos, and D. Y. Goswami, "Synthesis, characterization, and applications of ZnO Nanowires," *Journal of Nanomaterials,* p. 22, 2012.

[47] W. Zhao, X. Song, Z. Yin, C. Fan, G. Chen, S. Sun, "Self-assembly of ZnO nanosheets into nanoflowers at room temperature," *Materials Research Bulletin,* no. 43, pp. 3171-3176, 2008.

[48] D. Liu, W. Wu, Y. Qiu, S. Yang, S. Xiao, Q. Q. Wang, L. Ding, and J. Wang, "surface functionalization of ZnO nanotetrapods with photoactive and electro-active organic monolayers," *Langmuir ,* no. 24, pp. 5052-

5059 , 2008.

[49] http://ecee.colorado.edu, "bart/book/book/chapter2/ch2," 10 October 2014. [Online].

[50] F. C. Adams, and C. Barbante, "Nanoscience, nanotechnology and spectrometry," *Spectrochimica Acta Part B,* no. 86, pp. 3-13, 2013.

[51] V.Pokropivny et al, "Introduction to nanomaterials and Nanotechnology," pp. 1-37, 2007.

[52] Mahmad.S.B, "Synthesis and characterizaton of zinc oxide nanostructures," *Thesis submitted to University Sains Malasia,* pp. 3-27, 2008.

[53] Xiong HM, Liu DP, Xia YY, Chen JS, *Chem Mater 17:3062,* 2005.

[54] Xiong HM, Wang ZD, Xia YY, *Adv Mater 18:748,* 2006.

[55] Xiong HM, Xu Y, Ren OG, Xia YY , *J Am, Chem Soc 130 :7522,* 2008.

[56] Wang XD, Summers CJ, Wang ZL, *Nano Lett. 4 : 423,* 2004.

[57] Wang ZL, *ApplPhys A-Mater SciProc 88:7,* 2007.

[58] Djurisic AB, Ng AMC, Chen XY , *Prog Quantum Electron 34:191,* 2010.

[59] "http://en.wikipidia.org/Zinc Oxide.jpq," [Online].

[60] J.C. Johnson H. Yan, R.D. Schaller, L.H. Haber, R.J. Saykally, P. Yang, *Phys.chem.B 105 11387,* 2001.

[61] M.R. Hoffman, S.T. Martin, W. Choi, D.W. Bahneman, *Chem. Rev. 95 : 69,* 1995.

[62] O. Legrini, E. Oliveros, A.M. Braun , *Chem. Rev. 93 :671,* 1993.

[63] K. Kähler, M.C. Holz, M. Rohe, J. Strunk, M. Muhler, *Chem. Phys. Chem. 11 (12) : 2458,* 2010.

[64] S. Sá, H. Silva, L. Brandão, J.M. Sousa, A. Mendes, *Applied Catalysis B: Environmental 99 :43,* 2010.

[65] N. Saito, H. Haneda, K. Koumoto, *Adv. Mater. 14 : 418,* 2002.

[66] J. Liquianga Q. Yichun, W. Baiqi, L. Shudan, J. Baojiang, Y. Libin, F. Wei, F. Honggang, S, *Jiazhong, Solar Energy Materials & Solar Cells 90 :1773,* 2006.

[67] A. Dorfan, N. Kumar, J-in Hahm, Langmuir 22 :4890, 2006.

[68] M. Willander et, "Zinc oxide nanorod based photonic devices :recent progress in growth, light emitting diodes and lasers," *Nanotechnology,* no. 20, p. 40, 2009.

[69] A. Janotti and C. G. Van de Walle, "Fundamentals of zinc oxide as a semiconductor," *Rep. Prog. Phys,* no. 72, p. 29 pages, 2009.

[70] Ü. Özgür, Ya. I. Alivov, C. Liu, A. Teke, M. A. Reshchikov, S. Doan, V. Avrutin, S. J.Cho, and H. Morkoç, "A comprehensive review of ZnO materials and devices," *Journal of Applied Physics,* no. 98, 2005.

[71] Z. L. Wang, and W. Wu, "Piezotronics and piezo-phototronics: fundamentals and applications," *National Science Review ,* no. 1, pp. 62-90, 2014.

[72] S. J. Pearton, D. P. Norton, M. P. Ivill, A. F. Hebard, J. M. Zavada, W. M. Chen, and I.A. Bunyanova, "Ferromagnetism in transition-metal doped ZnO," *Journal of Electronic Materials,* vol. 36, no. 4, pp. 462-471, 2007.

[73] I. A. Buyanova, W. M. Chen, M. P. Ivill, R. Pate, D. P. Norton, S. J. Pearton, J. W.Dong, A. Osinsky, B. Hertog, A. M. Dabiran, and P. P. Chow, "Optical characterization of ZnMnO-based dilute magnetic semiconductor structures," *Journal of Vacuum Science & Technology B ,* no. 24, pp. 259-262, 2006.

[74] A. Gorzkowska-Sobas, A. Galeckas, M. F. Sunding, S. Diplas, and A. Yu. Kuznetsov, "An investigation of Fe-doped ZnO thin films grown by magnetron sputtering," *phys.Scr. T141 ,* p. 7pp, 2010.

[75] C. Liu, F. Yun, H. Morkoc, "Ferromagnetism of ZnO and GaN," *A review, Journal of materials science, Materials in Electronics ,* no. 16, pp. 555-597, 2005.

[76] S. J. Pearton, D. P. Norton, M. P. Ivill, A. F. Hebard, J. M. Zavada, W. M. Chen, and I.A. Buyanova, "ZnO doped with transition metal ions, IEEE Transactions on electron devices," vol. 54, no. 5, pp. 1040-1048, 2007.

[77] T. Diet, "Dilute magnetic semiconductors: Functional ferromagnets,Nature Materials," vol. 2, pp. 646-648,
2003.

[78] A. B. Djurisic, and Y. H. Leung, "Optical properties of ZnO nanostructures, Small," vol. 2, no. 8-9, pp. 944-961, 2006.

[79] Z. L. Wang, "Zinc oxide nanostructures: growth, properties and applications," *J.phys.Condens. Matter ,* vol. 16, pp. R829-R858, 2004.

[80] A. K. Radzimska, and T. Jesionowski, "Zinc oxide–from synthesis to application," *A review, Materials ,* vol. 7, pp. 2833-2881, 2014.

[81] C. Klingshirn, ZnO, "From basics towards applications," *Phys. Stat. Sol,* vol. 244, no. 9, pp. 3027-3073, 2007.

[82] C. Klingshirn, "ZnO: Material, physics and applications," *ChemPhysChem,* vol. 8, pp. 782-803, 2007.

[83] Z. L. Wang, "ZnO nanowire and nanobelt platform for nanotechnology," *Materials Science and Engineering,* vol. R 64, pp. 33-71, 2009.

[84] S.J. Pearton, D.P. Norton, K. Ip, Y.W. Heo, T. Steiner, "Recent progress in processing and properties of ZnO," *Progress in Materials Science,* vol. 50, pp. 293-340, 2005.

[85] S. Singh et al, "Structure, microstructure and physical properties of ZnO based materials in various forms: bulk, thin film and nano," *J. Phys. D: Appl. Phys,* vol. 40, pp. 6312-6327, 2007.

[86] Z. Fan and J. G. Lu, "Zinc Oxide Nanostructures: Synthesis and properties," *J. Nanosci Nanotechnol,* vol. 5,

pp. 1561-1573, 2005.

[87] J. Cui, "Zinc oxide nanowires, Materials Characterization," vol. 64, pp. 43-52 , 2012.

[88] C. Klingshirn, "ZnO: From basics towards applications," *Phys. Stat. Sol. (b) 244,* no. 9, pp. 3027-3073 , 2007.

[89] B. K. Meyer et al, "Bound exciton and donor‐acceptor pair recombinations in ZnO," *Phys. Stat. Sol. (b) 241,* no. 2, pp. 231-260 , 2004.

[90] R. Zhu and R. Yang, "Separation of the piezotronic and piezoresistive effects in a zinc oxide nanowire," *Nanotechnology 25 ,* no. 345702(6pp), 2014.

[91] http://serc.carleton.edu/research_education/geochemsheets/techniques/XRD.html, 10 october 2014. [Online].

[92] N. Shakti, P. S. Gupta, "Structural and optical properties of sol-gel prepared ZnO thin film," *Applied Physics Research ,* vol. 2, no. 1, pp. 19-28, 2010.

[93] "http://prism.mit.edu/xray/oldsite/training.htm#chronological," 10 october 2014. [Online].

[94] "http://www.absoluteastronomy.com/topics/X-ray_crystallography," 10 0ctober 2014. [Online].

[95] M. Birkholz, "Principles of X-ray Diffraction, Thin film analysis by X-ray scattering," *WILEY-VCH Verlag GmbH & Co. KGaA, Weinheim,* pp. 10-11, 2006.

[96] Cordaro, J.F., Y.Shim and J.E.May, "Structural and Optical properties of ZnO nanorodsprepared by chemical bath deposition method.," *J.Appl. phys. 60: 41-90,* 1986.

[97] Huang, M...,S.Mao, H.Feick, H.Yan, Y. Wu, H.Kind, E.Weber, R.Russo and P.Yang, "Electrodeposited ZnO films with high UV emission properties," *Science 292: 1897-9,* 2001.

[98] Pan, Z.R. Dai and Z.L Wang, "Nano belts of semiconductoring oxides," *Journal of Science 291 :1947-49,* 2001.

[99] "htt://www.scribd.com/doc/21053651/Electronic-spectroscopy-UV-visible," [Online].

[100] S.Monticone, R.Tufeu and A.V. Kanaev, "Complex nature of the UV and visible fluorescence of colloidal ZnO nanoparticles," *Journal of physic chemistry B,* vol. 102, pp. 2854, 1998, 1998.

[101] El-Kemary, M.,H. El-Shamy and I.El-Mehasseb, "Photo catalytic degradation of ciprofloxacin drug in water using ZnO nanoparticles," *Alloys Compd.433:237-240,* 2010.

[102] L.Guo, S. Yang, C.Yang, P. Yu, J. Wang, W. Ge, G. K. L. Wong, "Highly monodiperse polymercapped ZnO nano particles : Preparation and optical properties," *App. phys. Lett.,* vol. 76, p. 2901, 2000.

[103] S. Sambasivam et al, "Optical and ESR Studies on SnO2 Nanoparticles Doped with Dy3+ Ions," *Advanced Science Letters,* vol. 3, p. 465‐469, 2010.

[104] F. Bai, Pi. He, Z. Jia, X. Huang, Y. He, "Size-controlled preparation of monodispersed ZnO nanorods," *Materials Letters ,* vol. 59, pp. 1687-1690, 2005.

[105] LVJ., W.Gong, K. Huang, J. Zhu, F. Meng, X. Song and Z. Sun, "Effect of annealing temperature on photo-catalytic activity of ZnO thin films prepared by slo-gel method," *Supper lattice and Microstructures 50(2),* pp. 98-106, 2011.

[106] G. Murugadoss, "Synthesis and Characterization of Transition Metals Doped ZnO Nanorods," *J. Mater. Sci. Technol. 28(7),* pp. 587-593, 2012.

[107] B.L THERAJA, Modern physics, 2002, pp. 190-226.

[108] Zhang, Q., Dandeneau, C.S., Zhou, X., Cao, G.,, "ZnO nanostructures for dye-sensitized solar cells," *Adv. Mater,* no. 21, p. 4087–4108, 2009.

[109] Shah, S.M et al, "Optical and morphological studies of transition metal doped ZnO nanorods and their applications in hybride bulk heterojection solar cells.," *Arbian Journal of chemistry,* 2014.